UDC 627.824.2:699.841
IRSTI 67.11.59; 70.17.29
RESEARCH ARTICLE

ASSESSMENT OF THE TECHNICAL CONDITION OF A DAM LOCATED IN A SEISMICALLY ACTIVE ZONE

G.T. Kareken[1]*, N.I. Vatin[2], N.A. Shanshabayev[1,3], A.A. Bryantsev[1,4], S.Ye. Orazov[1]

[1]International Educational Corporation, 050043, Almaty, Kazakhstan
[2]Peter the Great St. Petersburg Polytechnic University (SPbPU), 195251, St. Petersburg, Russia
[3]LLP «StroyTechExpertiza», Taraz, Kazakhstan
[4]LLP «RAS Engineering Research Institute», Almaty, Kazakhstan

Abstract. *The aim of this study is to assess the technical condition of a dam in a seismically active zone of Kazakhstan. The object is the pressure front of the Sh. Chokin Kapchagay hydropower plant. It consists of a 52 m hydraulic-fill river-bed dam, a 56 m gravel-rubble ravine dam with a sandy-loam screen, and a quartz-porphyry rock abutment. The dams were designed for intensity 7 (MSK-64), but the site intensity was raised to 8 after the 1988 Spitak earthquake. The materials comprised the dynamic passports of the 2025 survey, settlement records and phreatic curves. The methods included in-situ P and S wave velocity profiling and pseudo-static slope-stability analysis. The seepage regime of both dams is stable. Mean settlement rates are 1.6-2.3 mm/yr for the river-bed dam and 2.06-3.8 mm/yr for the ravine dam, and relative compression does not exceed 0.010 %/yr. Wave velocities and dynamic modulus increase with depth without low-velocity zones. The intensely fractured upper 2 m of the abutment has half the compressive strength of deeper rock. All slopes meet the Class I stability requirements at intensities 7 and 8. At the check intensity of 9, the upstream slope of the ravine dam has K_s = 1.14, 3.4 % below the normative 1.18. It is concluded that settlement is decaying, although the ravine dam has not yet stabilised. The pressure front is stable at the current site intensity of 8, and the upstream slope of the ravine dam is its critical element. Dynamic-property profiles of these dams are published for the first time.*

Keywords: *hydraulic-fill dam; earthfill dam; seismic slope stability; shear-wave velocity; dynamic properties; long-term settlement; Kapchagay HPP.*

***Corresponding author**
Gulfairuz Kareken, e-mail: gulfairuz_1997@mail.ru

https://doi.org/10.51488/1680-080X/2026.3-21

ӘОЖ 627.824.2:699.841
ҒТАМР 67.11.59; 70.17.29
ҒЫЛЫМИ МАҚАЛА

СЕЙСМИКАЛЫҚ БЕЛСЕНДІ АЙМАҚТА ОРНАЛАСҚАН БӨГЕТТІҢ ТЕХНИКАЛЫҚ ЖАЙ-КҮЙІН БАҒАЛАУ

Г.Т. Қарекен[1]*, Н.И. Ватин[2], Н.А. Шаншабаев[1,3], А.А. Брянцев[1,4], С.Е. Оразов[1]

[1]Халықаралық білім беру корпорациясы, 050043, Алматы, Қазақстан
[2]Ұлы Петр атындағы Санкт-Петербург политехникалық университеті (СПбПУ), 195251, Санкт-Петербург, Ресей
[3]«СтройТехЭкспертиза» ЖШС, Тараз, Қазақстан
[4]«RAS Engineering» ғылыми-зерттеу институты» ЖШС, Алматы, Қазақстан

Аңдатпа. *Зерттеудің мақсаты - Қазақстанның сейсмикалық белсенді аймағында орналасқан бөгеттің техникалық жай-күйін бағалау. Зерттеу нысаны - Ш. Чокин атындағы Қапшағай СЭС-і. Ол биіктігі 52 м арналық шайылма бөгеттен, құмдақ экраны бар биіктігі 56 м жыралық бөгеттен және жартасты қалдық массивтен тұрады. Бөгеттер MSK-64 шкаласы бойынша 7 балдық сейсмикалыққа жобаланған, алайда 1988 жылғы Спитак жер сілкінісінен кейін алаңның сейсмикалығы 8 балға дейін арттырылды. Көпжылдық шөгуді бақылау деректері және 2025 жылғы зерттеу нәтижелері бойынша тұрғызылған депрессия қисықтары пайдаланылды. Бөгеттер денесінде бойлық және көлденең толқындардың жылдамдықтары анықталды. Еңістердің орнықтылығы 7, 8 және 9 балдық сейсмикалықта ВНИИГ-Терцаги әдісімен есептелді. Екі бөгеттің де сүзілу тәртібі тұрақты. Орташа шөгу жылдамдығы арналық бөгет үшін 1,6-2,3 мм/жыл, жыралық бөгет үшін 2,06-3,8 мм/жыл құрайды, ал салыстырмалы сығылу 0,02 %/жыл критерийі кезінде 0,010 %/жылдан аспайды. Толқындардың жылдамдығы мен динамикалық серпімділік модулі тереңдеген сайын артады, жылдамдығы төмен аймақтар анықталған жоқ. Қалдық массивтің 2 м тереңдікке дейінгі қатты жарықшақты аймағында жыныстардың сығылуға беріктігі массивтегіден екі есе төмен. 7 және 8 балдық сейсмикалықта барлық еңістер I класты құрылыстардың орнықтылық талаптарын қанағаттандырады. 9 балдық тексеру сейсмикалығында жыралық бөгеттің жоғарғы еңісінің орнықтылық коэффициенті K_s = 1,14, бұл 1,18 нормативтік мәнінен 3,4 %-ға төмен. Шөгу сөніп келеді, алайда жыралық бөгетте ол әлі тұрақтанбаған. Қазіргі 8 балдық сейсмикалығында орнықты, оның сыни элементі - жыралық бөгеттің жоғарғы еңісі. Бұл бөгеттердің динамикалық қасиеттері алғаш рет жарияланып отыр.*

Түйінді сөздер: *шайылма бөгет; экраны бар топырақ бөгет; еңістердің сейсмикалық орнықтылығы; көлденең толқындар жылдамдығы; динамикалық қасиеттер; көпжылдық шөгу; Қапшағай СЭС.*

***Автор-корреспондент**
Гүлфайруз Қарекен, e-mail: gulfairuz_1997@mail.ru

https://doi.org/10.51488/1680-080X/2026.3-21

УДК 627.824.2:699.841
МРНТИ 67.11.59; 70.17.29
НАУЧНАЯ СТАТЬЯ

ОЦЕНКА ТЕХНИЧЕСКОГО СОСТОЯНИЯ ПЛОТИНЫ, РАСПОЛОЖЕННОЙ В СЕЙСМИЧЕСКИ АКТИВНОЙ ЗОНЕ

Г.Т. Карекен[1]*, Н.И. Ватин[2], Н.А. Шаншабаев[1,3], А.А. Брянцев[1,4], С.Е. Оразов[1]

[1]Международная образовательная корпорация, 050043, Алматы, Казахстан
[2]Санкт-Петербургский политехнический университет Петра Великого (СПбПУ), 195251, Санкт-Петербург, Россия
[3]ТОО «СтройТехЭкспертиза», Тараз, Казахстан
[4]ТОО «Научно-исследовательский институт «Ras Engineering», Алматы, Казахстан

Аннотация. *Целью исследования является оценка технического состояния плотины в сейсмически активной зоне Казахстана. Объектом исследования является напорный фронт Капшагайской ГЭС им. Ш. Чокина. Он включает намывную русловую плотину высотой 52 м, логовую плотину высотой 56 м с супесчаным экраном и скальный останец. Плотины запроектированы на сейсмичность 7 баллов по шкале MSK-64. После Спитакского землетрясения 1988 г. сейсмичность площадки повышена до 8 баллов. Использованы данные многолетних наблюдений за осадками и кривые депрессии, построенные по результатам обследования 2025 г. Определены скорости продольных и поперечных волн в теле плотин. Устойчивость откосов рассчитана методом ВНИИГ-Терцаги при сейсмичности 7, 8 и 9 баллов. Фильтрационный режим обеих плотин стабилен. Средняя скорость осадок составляет 1,6-2,3 мм/год для русловой плотины и 2,06-3,8 мм/год для логовой; относительное сжатие не превышает 0,010 %/год при критерии 0,02 %/год. Скорости волн и динамический модуль упругости возрастают с глубиной, зон пониженных скоростей не выявлено. В интенсивно трещиноватой зоне останца до глубины 2 м прочность пород на сжатие вдвое ниже, чем в массиве. При сейсмичности 7 и 8 баллов все откосы удовлетворяют требованиям устойчивости для сооружений I класса. При поверочной сейсмичности 9 баллов коэффициент устойчивости верхового откоса логовой плотины K_s = 1,14, что на 3,4 % ниже нормативного значения 1,18. Сделан вывод, что осадки затухают, однако на логовой плотине они ещё не стабилизировались. Напорный фронт устойчив при текущей сейсмичности площадки 8 баллов; его критическим элементом является верховой откос логовой плотины. Профили динамических свойств этих плотин публикуются впервые.*

Ключевые слова: *намывная плотина; земляная плотина с экраном; сейсмическая устойчивость откосов; скорость поперечных волн; динамические свойства; многолетние осадки; Капшагайская ГЭС.*

***Автор-корреспондент**
Гульфайруз Карекен, e-mail: gulfairuz_1997@mail.ru

https://doi.org/10.51488/1680-080X/2026.3-21

1 INTRODUCTION

Embankment dams in seismic regions require periodic reassessment. Decades after construction, they must still meet their design assumptions. Seismic hazard estimates may also change during service. The design basis must then be checked against the new hazard.

The Sh. Chokin Kapchagay hydropower plant is located on the Ili River in the Almaty region of Kazakhstan. The reservoir volume adopted for classification of the structures is 18.6 km³. The reservoir has not been filled to its design capacity. The maximum volume, 16.4 km³, was reached during the first filling [1].

The pressure front has three elements. The first is a hydraulic-fill river-bed dam. The second is a gravel-rubble earthfill ravine dam. It has rock-fill loading berms and a low-permeability sandy-loam upstream screen. The third is a natural rock abutment. This quartz-porphyry ridge separates the river channel from a dry ravine. It houses the headrace tunnels and penstocks [2]. The plant has been in operation for more than 50 years.

Both dams were designed for an intensity of 7 on the MSK-64 scale. The seismic hazard maps of south-eastern Kazakhstan were revised after the Spitak earthquake. The site intensity was raised to 8 [3]. The safety declaration of the plant confirmed this value. The pressure front has thus operated for over three decades under a hazard above its design basis.

National regulations require three types of seismic surveillance for Class I hydraulic structures at sites of intensity 7 and above [4]. Seismometric monitoring records the response of the dams and abutments. Seismological monitoring records ground motion in the reservoir bed and adjacent areas. Periodic in-situ dynamic testing determines the natural frequencies, mode shapes and damping of the structures.

Ambient and forced-vibration tests are the usual tools for identifying the dynamic characteristics of dams. They have been applied to concrete dams [5,6] and embankment dams [7-9]. Conventional instrumentation remains the main tool for checking seepage and deformation [10]. It includes piezometers, settlement benchmarks, joint gauges and seepage weirs. Non-destructive methods complement it in detecting hidden defects. Ground-penetrating radar and 3D ultrasonic tomography have recently been applied to the earth dam and spillway of the Tasotkel reservoir in Kazakhstan [11,12]. Seismic surveys provide shear-wave velocity profiles [13]. Refraction, cross-hole and surface-wave methods are used for this purpose. These profiles yield the dynamic moduli needed for dynamic-response and pseudo-static slope-stability analyses [14].

Published data on the Kapchagay pressure front are limited. Earlier work studied the river-bed dam using records of two regional earthquakes [15]. It estimated the vibration period of the dam at 0.59-0.67 s. A recent study analysed the seismic response and frequency-dependent amplification of the river-bed dam from bedrock-to-crest earthquake records [16]. Related studies in Kazakhstan have addressed the seismic safety of structures [17], the degradation of concrete hydraulic structures [18], geodetic monitoring of vertical movements [19], slope stability [20] and weak foundations of embankments [21]. The dynamic properties of the dam materials, however, have not been published. The slope stability of both dams has been re-evaluated for the revised site intensity. This analysis exists only in the internal documentation of the plant. It has not been published in peer-reviewed form.

The study was carried out in 2025. It was based on the field and office investigation performed as the latest five-yearly update of the dynamic passports of the river-bed dam, the ravine dam and the rock abutment. The paper combines four types of evidence:

- long-term settlement and seepage records;
- in-situ profiles of compressional-wave (V_p) and shear-wave (V_s) velocities in both dams;
- geomechanical properties of the rock abutment;
- pseudo-static seismic slope-stability analysis.

The paper addresses the dynamic properties of the dam materials. The natural frequencies and damping of the structures are beyond its scope.

The novelty of the study is threefold. First, it presents the first published profiles of V_p, V_s,

https://doi.org/10.51488/1680-080X/2026.3-21

dynamic Poisson's ratio and dynamic modulus for both dams, to the authors' knowledge. No dynamic data have previously been published for the ravine dam. Second, it combines these properties with long-term settlement records and current seepage data in one assessment. Third, it re-evaluates the seismic slope stability of both dams under the revised site intensity. The analysis includes a check one intensity point higher. With the Class I reliability factor, the upstream slope of the ravine dam fails to meet the normative requirement at this check level. Together, these results form a documented baseline for a Class I pressure front after more than 50 years of operation in a seismic region.

The objectives of the study are: (i) to describe the instrumentation network and the testing methods; (ii) to present the seepage, settlement and seismic velocity data and the resulting dynamic properties of the dam materials; (iii) to re-evaluate the seismic slope stability of both dams at intensities 7 and 8 against the national safety factors for Class I structures, with a check at intensity 9; (iv) to assess the overall condition of the pressure front under the revised seismic classification of the site.

2 MATERIALS AND METHODS

2.1 Structures and site characterisation

The river-bed dam is a hydraulic-fill earth dam (Fig. 1). It is 52.0 m high and 470 m long. The crest is 21 m wide, at elevation (el.) 491.6 m. The base is 406 m wide. The dam body (zone 1) was hydraulically filled to a height of 49.0 m. It consists of fine-grained, uniform aeolian sand from borrow pit No. 3 (k = 2.5-5.0 m/day). Construction began in 1965. The dam was accepted into operation in December 1970.

The design provides seismic stability through flat slopes, rock-fill surcharges and loading berms. The surcharges are 3 m thick and cover both slopes. The upstream slope is 1:4 above a berm at el. 473.0 m and 1:5 below it. The downstream slope is 1:4 above a 5 m wide berm at el. 478.0 m and 1:5 below it.

The upstream loading berm (zone 2) consists of gravel-rubble soil from borrow pit No. 16 (k = 2.5-5.0 m/day). Its top is at el. 456.0 m. Rock fill (zone 3; k = 200 m/day) covers the berm and the upstream slope. The downstream loading berm (zone 4) is built of rock fill (k = 200 m/day). Its top is at el. 460.0 m, and its crest is 6 m wide. This berm also serves as a drainage prism. Three transition layers separate it from the dam body:

- zone 5: natural sand-gravel mix from borrow pit No. 9 (k = 35 m/day);
- zone 6: natural sand-gravel mix from the tailrace channel excavation (k = 40 m/day);
- zone 7: crushed stone, d = 0.2-8.0 mm (k = 200 m/day).

Sand from borrow pit No. 3b (zone 8; k = 2.5-5.0 m/day) surcharges the downstream slope and the crest. A 0.5 m layer of gravel-rubble soil (zone 9; k = 2.5-5.0 m/day) protects the downstream slope. Above el. 472.0 m, the upstream slope is faced with monolithic reinforced-concrete slabs (zone 10). The slabs are 10 × 10 m in plan and 0.20-0.30 m thick and rest on a crushed-stone bed. Containment dykes (zone 11) of dry-placed sand from borrow pit No. 3 bound the hydraulic-fill zone.

The dam rests mainly on alluvial gravel-pebble soil and gravelly sand. This layer is 5-20 m thick, with an average k of 35 m/day. Bedrock under the river channel lies at el. 423.0-424.0 m. At the upstream left-bank contact, the foundation includes aeolian deposits 8 m thick (k = 5.0 m/day). Both abutments consist of strong but fractured quartz porphyry. The left abutment is the rock ridge (k = 0.02 m/day). The right abutment is a near-vertical bedrock slope (k = 0.03 m/day).

A collector in the downstream berm intercepts seepage through the dam. It is 195 m long and has a gradient of 0.001. It consists of reinforced-concrete pipes 1.5 m in diameter. Two outlet collectors, 80 m and 100 m long, discharge the flow into the tailrace channel. The pipe network was designed for a seepage discharge of 3.0 m^3/s.

https://doi.org/10.51488/1680-080X/2026.3-21

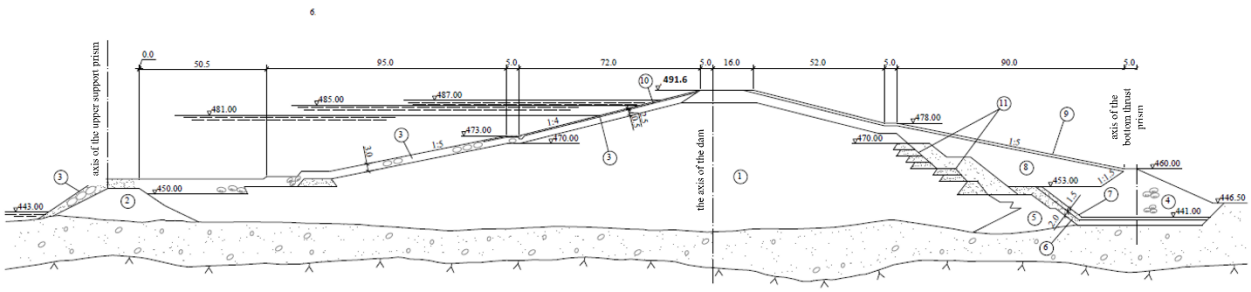

Figure 1 - Typical cross-section of the river-bed dam (zones 1-11 are described in the text) [Author's material]

The ravine dam is an earthfill dam with an upstream screen (Fig. 2). Its height is 56.0 m from the base of the screen. The crest is 370 m long and 10 m wide. It lies at el. 491.0 m. The base is 270 m wide.

The foundation consists of proluvial-deluvial deposits: gravel-rubble soil, sandy loam and sand. Their average k is 35 m/day. Both flanks abut rock. The right flank abuts the quartz-porphyry ridge. The same ridge forms the left abutment of the river-bed dam.

The first-stage dam body (zone 4a) consists of soil from the supply-channel excavation (k = 2.5-5.0 m/day). Two upstream wedges enlarge it:

- zone 4: gravel-rubble soil from borrow pit No. 16 (k = 2.5-5.0 m/day);
- zone 5: sand from borrow pit No. 3b (k = 3.4 m/day).

The upstream screen (zone 6) consists of sandy loam and sand from the spoil bank. Its k is 0.5 m/day, five to ten times lower than that of the dam body. A cut-off key connects the screen to the rock. The key contains a transition layer of sand-gravel mix from borrow pit No. 9 (zone 11; k = 35 m/day). Blanket grouting (zone 13) treats the foundation beneath the key to a depth of 30 m. A concrete cap (zone 12) covers the grouted zone.

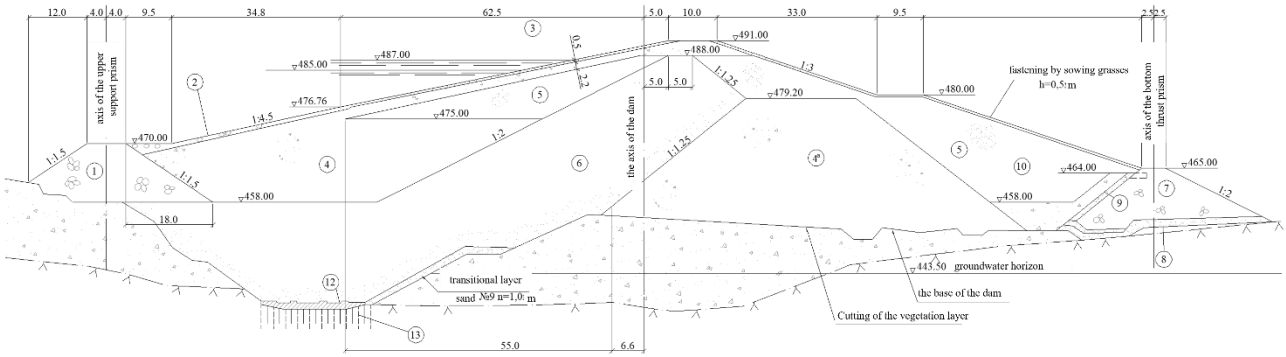

Figure 2 - Typical cross-section of the ravine dam (zones 1-13 are described in the text) [Author's material]

Flat slopes and rock-fill loading berms provide seismic stability. The upstream slope is 1:5. The upstream berm (zone 1) and the slope protection (zone 2) are rock fill (k = 200 m/day). Above el. 476.96 m, monolithic reinforced-concrete slabs face the slope (zone 3). The slabs are 10 × 10 m in plan and 0.20 m thick. They rest on a crushed-stone filter. Joints divide the facing into 40 m sections. Below el. 476.96 m, rock fill 1.0 m thick protects the slope.

The downstream slope is 1:3. A berm 9.5 m wide lies at el. 480.0 m. Gravel-rubble soil seeded with grass protects the slope. The downstream berm (zone 7; k = 200 m/day) is rock fill. It also serves as a drainage prism. Its top is at el. 465.0 m. Its crest is 5 m wide. The berm rests on sand-gravel mix from borrow pit No. 9 (zone 8; k = 35 m/day). Gravel-rubble soil from borrow pit No. 16 forms the transition between the berm and the dam body (zone 10; k = 2.5-5.0 m/day). A crushed-stone layer with d = 0.2-80 mm completes the filter (zone 9; k = 200 m/day).

Perforated asbestos-cement pipes 0.5 m in diameter collect seepage in the prism. Inspection wells give access to the drains. A reinforced-concrete pipe 1.0 m in diameter discharges the flow into

https://doi.org/10.51488/1680-080X/2026.3-21

the Ili River. A triangular weir in the outlet well measures the discharge. The design seepage discharge is 1.5 m³/s.

The rock abutment is an elongated ridge. It separates the Ili River channel from the dry ravine. The survey documentation uses two names for the rock: porphyrite for the massif and its dykes, and porphyry at the dam contacts. This paper uses "quartz porphyry" throughout. The rock is strong but fractured, locally intensely fractured. The ridge is 73.0 m high. Its base is 150 m long. Its crest reaches el. 504.3 m. At el. 479.0 m, the ridge is 50-70 m wide. It forms 460 m of the pressure front.

The ridge hosts two inclined operating tunnels, four penstocks, a transport adit and a drainage adit. The drainage adit runs on the downstream side, 30 m from the unit axis. Its floor lies at el. 454.0 m, with a gradient of 0.007. The adit is 382 m long. Its cross-section is 3.0 × 3.6 m. Two outlet branches, 85 m long in total, discharge the seepage. Drainage boreholes 105 mm in diameter were drilled from the adit at 2.5 m spacing. The upper boreholes reach el. 485.0 m. The lower boreholes are 40 m deep.

A grout curtain runs between the drainage adit and the water intake, 10 m from the adit. Its depth is 15-68 m. The hole spacing is 3 m. The seepage water attacks ordinary cement with sulfates. Sulfate-resistant Portland cement (grade 400) was therefore used. These measures lower the seepage level. They also restore the integrity of the rock mass disturbed during construction.

SN RK 3.04-01-2023 "Hydraulic Structures" sets three criteria for the class of a hydraulic structure [4]:

- height and foundation type;
- socio-economic responsibility;
- consequences of a hydrodynamic accident.

The most severe class governs [4]. By socio-economic responsibility, the Kapchagay dams are Class I. This class follows from the reservoir volume of 18.6 km³. More than 3000 permanent residents live in the potential inundation zone. The consequences criterion therefore also gives Class I. Both dams are thus Class I structures, the highest class in the national code. The rock abutment belongs to the same pressure front. It therefore takes the same class [4] (Table 1).

The original design assumed a seismic intensity of 7 (MSK-64). The seismic zoning maps were revised after the Spitak earthquake. The site intensity was then raised to 8. The safety declaration of the Kapchagay HPP confirmed this value. The stability analyses performed in 2025 followed SP RK 2.03-30-2017 [22]. They considered three intensity levels: 7 (design), 8 (analysis) and 9 (check) (Table 1).

Table 1 – Principal geometric and classification parameters of the three structural elements [Author's material]

Parameter	River-bed dam	Ravine dam	Rock abutment
Type	Hydraulic-fill earth dam	Earthfill dam with upstream screen and rock-fill berms	Natural rock ridge
Maximum height, m	52.0	56.0 (from screen base)	73.0
Crest elevation, m (Baltic system)	491.6	491.0	504.3
Crest length, m	470.0	370.0	460.0 (along pressure front)
Crest width, m	21.0	10.0	50-70 (at el. 479.0)
Base dimension, m	406.0 (width)	270.0 (width)	150.0 (length)
Foundation	Alluvial gravel-pebble soil and gravelly sand, k ≈ 35 m/day	Proluvial-deluvial gravel-rubble soil, sandy loam and sand, k ≈ 35 m/day	Quartz porphyry
Seismicity (MSK-64): design / analysis / check-level	7 / 8 / 9	7 / 8 / 9	8
Structure class (SN RK 3.04-01-2023)	I	I	I

https://doi.org/10.51488/1680-080X/2026.3-21

2.2 Instrumentation network and monitoring regime

The pressure front is instrumented with standpipe piezometers, surface (SB) and deep (DB) settlement benchmarks, automated joint gauges, ultrasonic level gauges and pressure sensors (Table 2).

The river-bed dam has three monitoring sections. They contain 7, 7 and 6 working piezometers. Sections 1, 2 and 3 have four, four and two deep benchmarks, respectively. Each section has two surface benchmarks. Two more piezometers are installed at the right abutment. The rock abutment has 16 working piezometers and three surface benchmarks. The ravine dam has six monitoring sections. They contain 2, 3, 4, 3, 1 and 3 piezometers. Each section has two to five surface and three to five deep benchmarks. The pressure front thus has 54 working piezometers: 22 on the river-bed dam, 16 on the rock abutment and 16 on the ravine dam. Settlement observations began in 1976.

Until 2017, piezometric levels were measured manually with a dip meter. The readings were recorded in operating logs. An automated safety-monitoring system was commissioned in December 2016. It includes 51 LMP 307i pressure transducers (BD Sensors RUS). The transducers are installed in the piezometer standpipes. Each one converts water pressure into a standard output signal. The sensor and its electronic converter share a sealed steel or polymer housing. A vented cable supplies the atmospheric reference pressure. The transducers withstand repeated shocks of 1000 m/s² lasting 11 ms. This rating far exceeds the ground accelerations expected at the site.

Six Radon VB-Shch microprocessor gauges measure the opening of temperature-settlement joints. Three gauges are in the HPP building at el. 446.0 m (Fig. 3a). Three are on the water intake (Fig. 3b). Each gauge converts joint opening into an electrical signal. The signal is digitised and stored in non-volatile memory. The gauge consists of a measurement module, a support, a reference element, a gauge rod and a sealed cable gland. A vernier tongue allows manual checks with a caliper. Three reference points, A, B and C, are fixed at each gauge (Fig. 3). Points B and C lie on one side of the joint. The baseline BC (a) is therefore constant. Point A lies on the other side. Changes in AC (b) and AB (c) define the joint movement.

Two UU-60 ultrasonic gauges measure the headwater and tailwater levels without contact. The headwater gauge is at the intake of hydro-unit No. 1. The tailwater gauge is at the outlet of operational spillway No. 1. Two 415M pressure sensors measure the seepage head in the rock abutment. They are installed in the left wing of the drainage adit. All signals reach a dispatch point in the operations building online.

During the 2025 survey, part of the system was out of service:

- 23 of the 51 pressure transducers;
- both level gauges;
- one joint gauge (section 5a-5a).

The 470 m communication line to the tailwater gauge was also cut. The instrumental record is long but has gaps. This study therefore combines the manual records (up to 2017) with the automated data (from 2017 onwards).

This survey is the latest five-yearly update of the dynamic passports. After five decades of operation, the settlement and seepage of the dams change slowly. The reported trends are therefore expected to remain representative until the next five-yearly update.

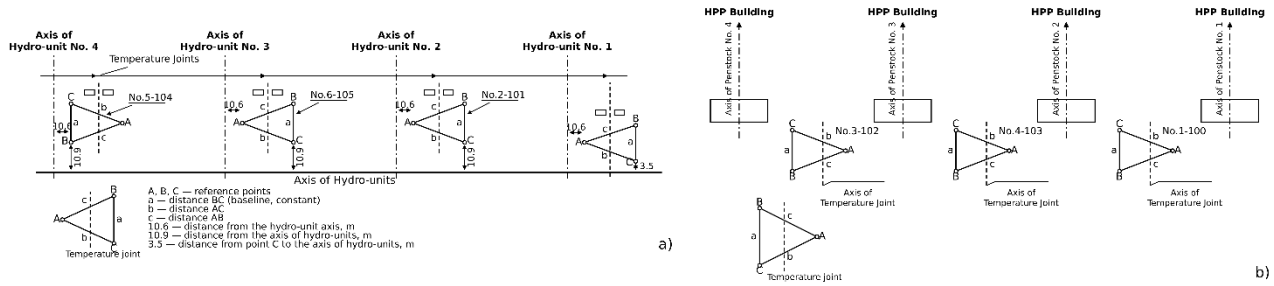

Figure 3 – Layout of the Radon VB-Shch joint gauges with reference points A, B and C: (a) HPP building, el. 446.0 m; (b) water intake [Author's material]

https://doi.org/10.51488/1680-080X/2026.3-21

Table 2 - Summary of the instrumentation network [Author's material]

Instrument	Quantity	Location
Standpipe piezometers	22 (7 + 7 + 6 in Sections 1-3; 2 at the right abutment)	River-bed dam
Standpipe piezometers	16	Rock abutment
Standpipe piezometers	16 (2 + 3 + 4 + 3 + 1 + 3 in Sections 1-6)	Ravine dam
Standpipe piezometers, total	54	Pressure front
Surface settlement benchmarks	2 per section (river-bed dam); 2-5 per section (ravine dam); 3 (rock abutment)	Crests, berms, rock abutment
Deep settlement benchmarks	4 per section (river-bed dam); 3-5 per section (ravine dam)	Dam bodies
Pressure transducers LMP 307i (BD Sensors RUS)	51, installed in December 2016	Piezometer standpipes of both dams and the rock abutment
Automated joint gauges Radon VB-Shch	6 (3 + 3)	HPP building (el. 446.0 m) and water intake
Ultrasonic level gauges UU-60	2	Headwater (intake of hydro-unit No. 1) and tailwater (outlet of spillway No. 1)
Pressure sensors 415M	2	Left wing of the drainage adit, rock abutment

2.3 Seepage and settlement monitoring

Seepage was assessed from phreatic curves at instrumented cross-sections. On the river-bed dam, curves were plotted for Sections 2 (PK 2+50) and 3 (PK 3+50). On the ravine dam, curves were plotted for Sections 3 (PK 1+89.5) and 4 (PK 2+39.5). On both dams, heads were measured in September and December. The head loss in each zone was also estimated. During the survey, the reservoir was about 6.4 m below the normal pool level. As a result, some piezometers in the upstream wedge of the ravine dam were dry.

Settlement has been monitored since 1976. Surface and deep benchmarks are installed on the crests and berms of both dams. Numerical records are available from 1995 onwards. The benchmarks with the largest settlement were used to assess the current trend. Nine such benchmarks were selected on the river-bed dam and 17 on the ravine dam. For each benchmark, the mean annual settlement rate was calculated for the last two decades of observations. This rate is the settlement increment divided by the length of the interval. The range and the average rate were then found for each dam. Recommendations P 87-2001 [23] associate the stabilisation of settlement with a rate of about 1-2 mm/yr (Section 5.12). This value was used here as a reference.

Relative compression provided a second check. The annual settlement rate was divided by the thickness of the compressible layer under the crest. Only the fill was treated as compressible. This assumption is conservative, because a thinner layer gives a higher relative compression. For the river-bed dam, the layer is the hydraulic-fill body, 52 m thick. For the ravine dam, it is the embankment fill above the alluvium, about 40 m thick. The survey report adopted a relative compression rate below 0.02 %/yr as the practical criterion of decaying settlement. This criterion was also used here.

2.4 Dynamic passports

Class I hydraulic structures at sites of seismic intensity 7 and above require seismic monitoring and dynamic testing [4]. Dynamic passports of the river-bed dam, the ravine dam and the rock abutment were compiled during the 2025 survey. Under the national operating rules, the dynamic passports of hydraulic structures are updated every five years [24]. These passports are therefore the current ones.

For each dam, the passports give depth profiles of the compressional-wave (V_p) and shear-wave (V_s) velocities, the dynamic Poisson's ratio ν and the dynamic modulus Ed. The profiles were obtained at three verticals on each dam. On the river-bed dam, the verticals are on the crest (el. 491.6 m), the berm (el. 478.0 m) and the downstream slope (el. 468.0 m). On the ravine dam, they are on the crest (el. 491.0 m), the berm (el. 480.0 m) and the downstream loading berm (el. 465.0 m). The profiles

https://doi.org/10.51488/1680-080X/2026.3-21

reach 21-23 m on the river-bed dam and 18-42 m on the ravine dam. They define the material zones of both dams. Below the phreatic surface, ν approaches 0.45-0.475.

The rock abutment is described by the physico-mechanical properties of quartz porphyry. These are density, compressive strength, elastic modulus, Poisson's ratio, friction angle and cohesion. They are given for two degrees of fracturing.

2.5 Seismic slope-stability analysis

The seismic stability of the upstream and downstream slopes of both dams was evaluated for circular slip surfaces. The VNIIG-Terzaghi method of slices was used. It is implemented in the Grot software (Hydroproject Institute, Moscow). This is a pseudo-static limit-equilibrium method. It is similar to the circular-slip methods widely used for embankment dams [14]. The analysis followed SP RK 2.03-30-2017 [22].

Stability is ensured if the most unfavourable slip surface satisfies

$$\gamma_{fc} \cdot F(\gamma_f) \leq \left(\frac{\gamma_c}{\gamma_n}\right) \cdot R\left(\frac{1}{\gamma_g}\right) \quad (1)$$

where:

F is the design destabilising force, the resultant moment of the active forces;

R is the design resisting force;

γ_f is the load reliability factor;

γ_g is the soil reliability factor;

γ_n is the reliability factor for the responsibility class;

γ_c is the working-conditions factor.

The stability factor is therefore

$$K_s = \frac{R}{F} \geq \frac{(\gamma_n \cdot \gamma_{fc})}{\gamma_c} \quad (2)$$

For Class I structures, γ_n = 1.25. The factor γ_{fc} is 1.00 for the basic combination and 0.90 for the special (seismic) combination. For the simplified method, γ_c = 0.95. Equation (2) then gives minimum stability factors of 1.32 for the basic combination and 1.18 for the special combination

The typical cross-sections of maximum height were analysed. The natural and saturated unit weights, cohesion and friction angle of each zone were taken from the dynamic passports. The hydraulic conductivities were taken from the design cross-sections (Figs. 1 and 2). The elastic properties were also taken from the passports. For the river-bed dam, E = 400 MPa and ν = 0.23. For the ravine dam, E = 800 MPa and ν = 0.25. The software computes the phreatic surface from the headwater and tailwater levels and the hydraulic conductivities.

Two load combinations were analysed for each slope. The basic combination includes the reservoir at the normal pool level (el. 485.0 m), steady seepage through the dam and the tailwater at el. 443.0 m. For the upstream slope, it also includes seepage forces from unsteady flow at the maximum possible drawdown rate. The special combination adds seismic loading of intensity 7, 8 and 9 to the basic combination. During the survey, the headwater was about 6.4 m below the normal pool level. The computed stability factors are therefore conservative for current operating conditions.

3 RESULTS AND DISCUSSION

3.1 Seepage regime

Piezometric records for the past decade show a stable seepage regime in both dams. On the river-bed dam, heads in the central zone and the downstream wedge have remained practically unchanged. Piezometers in the upstream wedge follow reservoir-level fluctuations. On the ravine dam, levels in the working piezometers have also remained stable in recent years.

Phreatic curves for the river-bed dam were constructed for Sections 2 (PK 2+50) and 3 (PK 3+50) (Figs. 4 and 5). Phreatic curves for the ravine dam were constructed for Sections 3 (PK 1+89.5)

https://doi.org/10.51488/1680-080X/2026.3-21

and 4 (PK 2+39.5) (Fig. 6). All curves are based on two piezometric surveys made in September and December. The headwater level was 478.61 m in September and 478.59 m in December. The tailwater level was 443.55 m and 443.34 m, respectively. The two surveys were made at almost the same headwater level. Their curves therefore characterise the seepage regime at one reservoir stage.

In all sections, the piezometric head decreases from the upstream to the downstream face. The largest head loss occurs in the upstream part of each dam. During the survey, the headwater was about 6.4 m below the normal pool level (el. 478.6 m against el. 485.0 m). Some piezometers in the upstream wedge of the ravine dam were therefore dry.

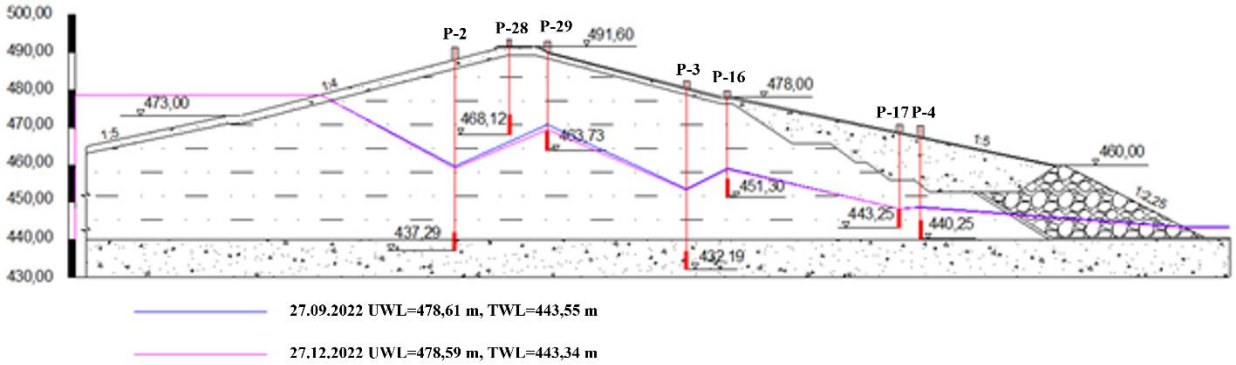

Figure 4 - Phreatic curves in Section 2 (PK 2+50) of the river-bed dam [Author's material]

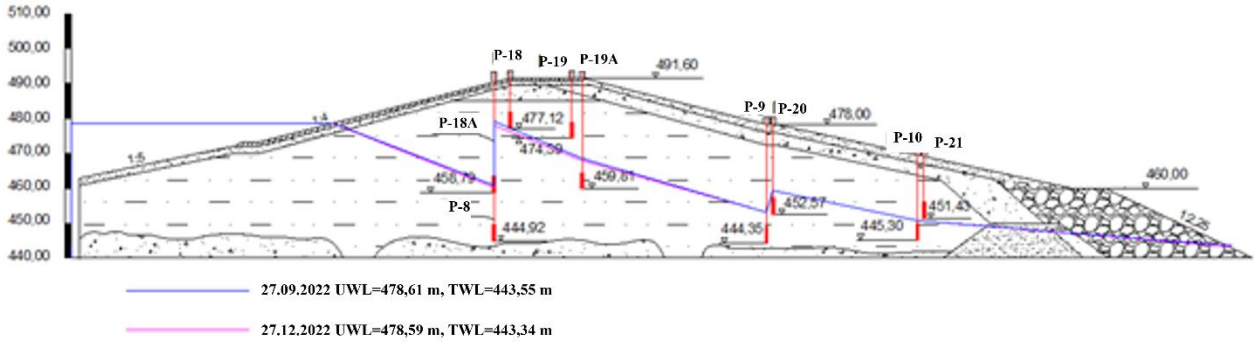

Figure 5 - Phreatic curves in Section 3 (PK 3+50) of the river-bed dam [Author's material]

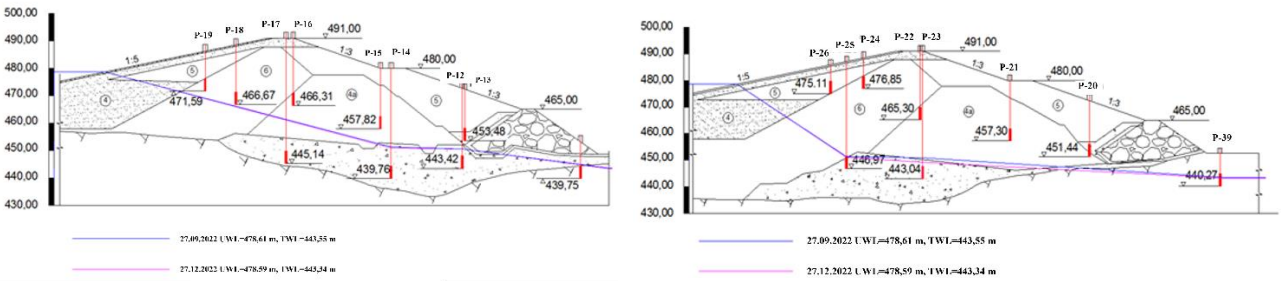

a) b)

Figure 6 - Phreatic curves in the ravine dam: (a) Section 3 (PK 1+89.5); (b) Section 4 (PK 2+39.5) [Author's material]

3.2 Settlement

Settlement is monitored by SB and DB benchmarks on the crests and berms of both dams. The river-bed dam has three monitoring sections. The ravine dam has six. Observations began in 1976. Numerical records are available from 1995 onwards.

Since 1976, the benchmarks of the river-bed dam still in service have settled by 1-96 mm. The maximum was recorded at DB-5. SB-3 had settled by about 151 mm before its observations stopped

https://doi.org/10.51488/1680-080X/2026.3-21

in 2012. The ravine dam settled by 1-210 mm. The maximum was recorded at SB-3. At most benchmarks, the total settlement does not exceed 100-151 mm. Over the full record, the largest settlement in each section was recorded at a surface benchmark (SB-1, SB-3 and SB-5) before 2012. Among the benchmarks still in service, the largest values are at deep benchmarks (DB-3, DB-5 and DB-11). At all benchmarks, settlement decays with time.

Over the last two observation years, the vertical movements of the river-bed dam benchmarks ranged from -2 mm (settlement) to +2 mm (rise). On the ravine dam, they ranged from -3 to +2 mm. The rises are within the measurement accuracy.

Table 3 - Settlement of the river-bed and ravine dams [Author's material]

Dam	Selected benchmarks	Total settlement 1976-2022, mm	Mean annual rate 2000-2022, mm/yr: range (mean)	Annual settlement 2021–2022, mm	Relative compression, %/yr: range (mean)
River-bed	9	91-96 (151 at SB-3 by 2012)	1.6-2.3 (1.96)	-2 to +2	0.003-0.004 (0.004)
Ravine	17	1-210	2.06-3.8 (2.96)	-3 to +2	0.005-0.010 (0.007)
Criterion	-	-	≈ 1-2 [24]	-	< 0.02

The current trend was assessed over the last two decades of observations. Only the benchmarks with the largest settlement were used. On the river-bed dam, nine benchmarks were selected: SB-1 to SB-4, DB-1, DB-5, DB-7, DB-8 and DB-11. SB-1, SB-3 and SB-5 were not observed in 2013-2016. In 2013, a solid fence of split blocks was built on the crest. The fence blocked the line of sight from the reference pillar OP-1, and the pillar was destroyed. In 2016, OP-1 was relocated. The three benchmarks were reinstalled in the same year.

For these benchmarks, the mean annual settlement rates are 1.6-2.3 mm/yr. Their average is 1.96 mm/yr. On the ravine dam, 17 benchmarks were selected: DB-1 to DB-5, DB-10, DB-11, DB-20, DB-25, DB-27, DB-31, SB-7, SB-8, SB-11, SB-12, SB-17 and SB-25. Their mean rates are 2.06-3.8 mm/yr. The average is 2.96 mm/yr (Table 3). On the river-bed dam, the average rate of 1.96 mm/yr lies at the upper bound of the 1-2 mm/yr reference [23]. The ravine dam settles faster. Its rates exceed the reference value.

Relative compression was estimated for the least favourable case. For the river-bed dam, the compressible layer was the 52 m hydraulic fill under the crest. For the ravine dam, it was the 40 m embankment above the alluvium. The relative compression rate is 0.003-0.004 %/yr for the river-bed dam. It is 0.005-0.010 %/yr for the ravine dam. Both values are well below 0.02 %/yr, the practical criterion adopted in the survey report. On both dams, the rates decrease with time. The settlement is therefore decaying. The ravine dam, however, has not yet reached the stabilisation level.

The three monitoring sections of the river-bed dam are described below (Fig. 7).

In Section 1 (Fig. 7a), SB-1 settled most. It reached about 100 mm by 2012. SB-2 has reached 79 mm. The deep benchmarks settled by 19 mm (DB-2), 24 mm (DB-4), 83 mm (DB-1) and 87 mm (DB-3). From 1976 to 1995, the benchmarks settled by about 5-70 mm. After 1995, the rate decreased at all benchmarks. From 2018 to 2021, DB-4, DB-3 and SB-2 rose by 9-13 mm.

Section 2 (Fig. 7b) shows the widest range of settlement. SB-3 settled by about 125 mm before 1995. By 2012, it reached about 151 mm. This is the largest value on the river-bed dam. The other benchmarks settled less: DB-5 by 96 mm, SB-4 by 72 mm, DB-7 by 62 mm, DB-6 by 31 mm and DB-8 by 19 mm. After 1995, the curves flatten. From 2018 to 2021, SB-4, DB-8 and DB-7 rose by 10–18 mm. The large settlement of SB-3 may indicate a locally more compressible zone in the fill or foundation. The available data cannot confirm this.

In Section 3 (Fig. 7c), SB-5 settled most. It reached about 84 mm by 1995 and about 102 mm by 2012. SB-6 and DB-11 settled gradually until 2006. By then, they had reached about 32 mm and 34 mm. In 2006-2007, both showed abrupt steps. SB-6 moved from about 32 to 68 mm. DB-11 moved from about 34 to 51 mm. By 2014, they reached about 79 mm and 61 mm. In 2015, both rose. SB-6

https://doi.org/10.51488/1680-080X/2026.3-21

rose by about 42 mm and DB-11 by about 14 mm. DB-12 settled least, by 5-26 mm over the whole period. After 2015, all benchmarks in this section are stable.

The ravine dam also showed rises of 6-13 mm in 2018-2021, for example at DB-1, DB-3 and SB-1. Simultaneous rises on both dams are unlikely to be real heave. The steps of 2006-2007 and 2015 are also atypical for a dam in service for several decades. They more likely reflect changes in the observation network or reference benchmarks. This should be verified against the survey logs.

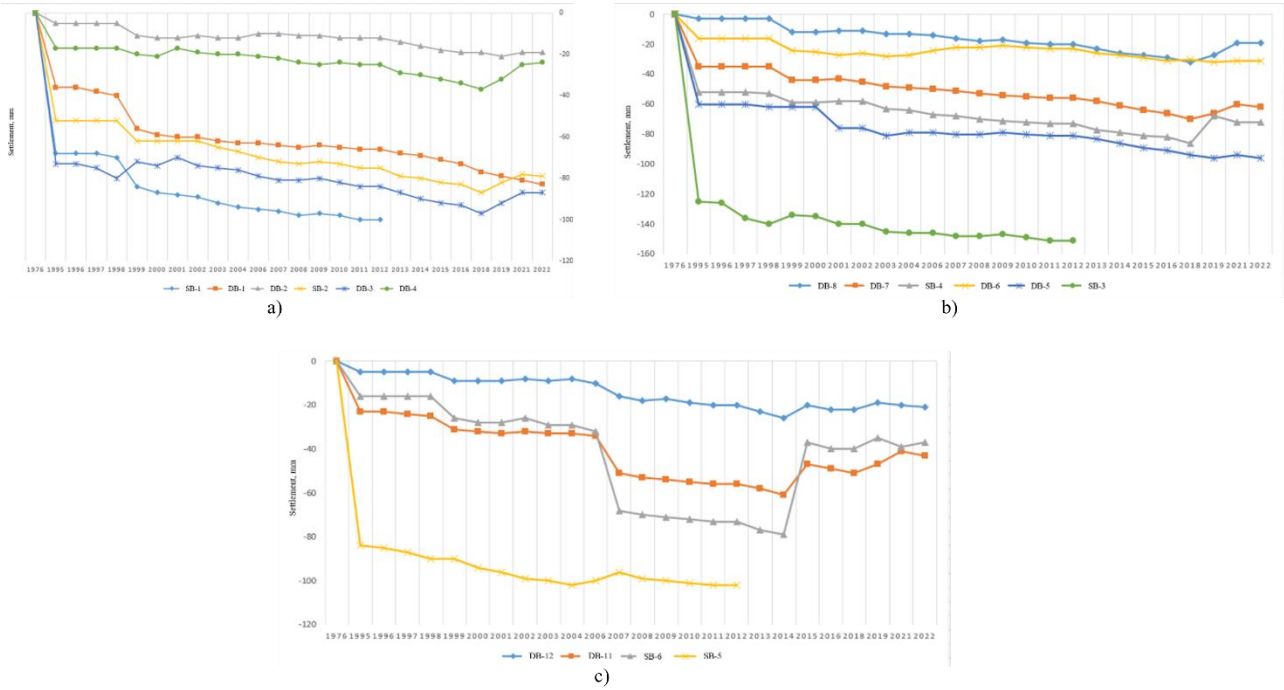

Figure 7 - Settlement of the river-bed dam benchmarks: (a) Section 1; (b) Section 2; (c) Section 3. The time axis is not to scale for 1976–1995 [Author's material]

3.3 Dynamic properties of the dam materials

V_p and V_s increase with depth at every vertical. This reflects the growing confining stress. At the deepest levels, the increase also marks the transition to saturated material.

Table 4 - Dynamic properties of the dam materials [Author's material]

Structure / zone	Depth, m	V_p, m/s	V_s, m/s	ν	E_d, MPa
River-bed dam, crest (hydraulic-fill sand)	1-22	340-520	205-300	0.22-0.24	150-340
River-bed dam, crest, saturated sand	23	1570	350	0.475	660
River-bed dam, berm (hydraulic-fill sand)	4-20	400-650	240-380	0.22-0.24	220-550
River-bed dam, berm, saturated sand	21	1570	400	0.47	780
River-bed dam, downstream slope (fill sand, gravel-rubble soil)	0-10	300-750	180-435	0.22-0.24	130-800
River-bed dam, downstream slope, saturated sand-gravel	21	1570	450	0.46	1080
Ravine dam, crest (sand, screen, gravel-rubble soil)	2-40	360-920	220-525	0.22-0.26	190-1220
Ravine dam, crest, saturated foundation	42	1900	570	0.45	1920
Ravine dam, berm	1-30	360-840	220-490	0.22-0.24	190-1060
Ravine dam, berm, saturated foundation	31	1900	570	0.45	1920
Ravine dam, downstream loading berm (rock fill)	2-10	440-680	240-340	0.29-0.33	290-630
Ravine dam, downstream loading berm, sand-grus soil	14	830	430	0.31	810
Ravine dam, downstream loading berm, saturated	18	1900	570	0.45	1920

https://doi.org/10.51488/1680-080X/2026.3-21

Fig. 8 shows the depth profiles of V_p (a) and E_d (b) for the river-bed dam. Curve 1 refers to the hydraulic-fill sand beneath the crest. Curve 2 refers to the hydraulic-fill sand beneath the berm. Curve 3 refers to the downstream slope. There, fill sand overlies gravel-rubble soil. E_d is given in 10^3 kgf/cm² ($1 \cdot 10^3$ kgf/cm² ≈ 98.1 MPa).

Beneath the crest, V_p increases from 340 m/s at 1 m to 520 m/s at 22 m. V_s increases from 205 to 300 m/s. ν increases from 0.22 to 0.24. E_d increases from about 150 to 340 MPa. At 23 m, the sand is saturated. V_p rises abruptly to 1570 m/s, and ν to 0.475. In saturated sand, the compressional wave travels mainly through the pore water. V_s (350 m/s) still reflects the soil skeleton.

The berm vertical shows a similar pattern. Between 4 and 20 m, V_p increases from 400 to 650 m/s. ν remains 0.22-0.24. At 21 m, V_p reaches 1570 m/s and ν 0.47. On the downstream slope, V_p increases from 300 m/s at the surface to 750 m/s at 10 m. At 21 m, V_p reaches 1570 m/s and ν 0.46. Beneath the crest and berm, V_p and E_d increase steadily with depth in the unsaturated zone. The hydraulic fill is therefore uniform.

Fig. 9 shows the same profiles for the ravine dam. Curve 1 refers to the sand-sandy-loam soil with grus beneath the crest. Curve 2 refers to the sand with grus beneath the berm. Curve 3 refers to the rock fill of the downstream loading berm.

Beneath the crest, V_p increases from 360 m/s at 2 m to 920 m/s at 40 m. The profile crosses the aeolian sand, the sandy-loam screen and the gravel-rubble soil. E_d increases from about 190 to 1220 MPa. In the saturated foundation, V_p rises to 1900 m/s and ν to 0.45. This transition lies at 42 m beneath the crest. Beneath the berm, it lies at 31 m. Beneath the downstream loading berm, it lies at 18 m.

In the rock fill (2-10 m), V_p is 440-680 m/s and V_s is 240-340 m/s. ν is 0.29-0.33. In the sand and gravel-rubble zones, ν is lower, 0.22-0.26 (Table 4). At equal depth, velocities and moduli are higher than on the river-bed dam. At 35-40 m, V_p reaches 870-920 m/s and E_d 1.1-1.2 GPa. The coarser gravel-rubble soils of the ravine dam explain this difference.

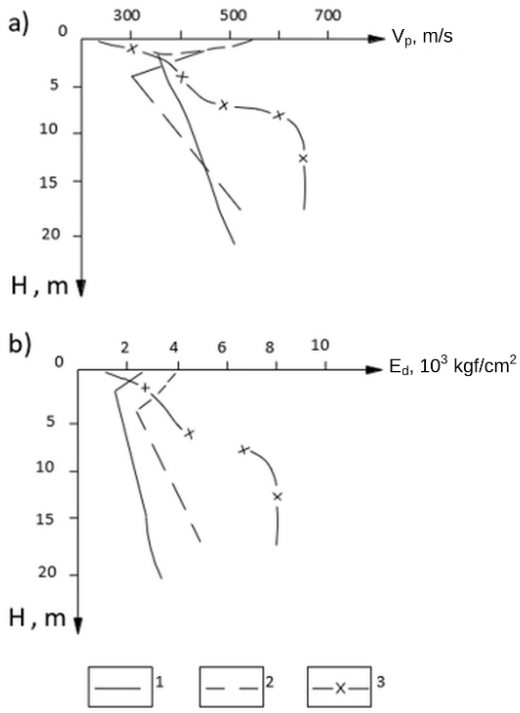

Figure 8 - Depth profiles at the river-bed dam: (a) V_p; (b) E_d [Author's material]

https://doi.org/10.51488/1680-080X/2026.3-21

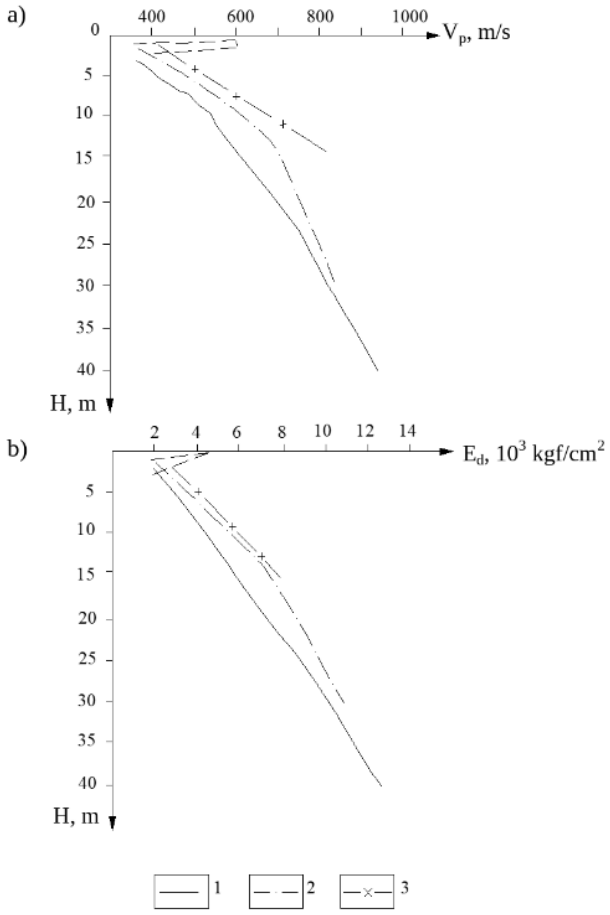

Figure 9 - Depth profiles at the ravine dam: (a) V_p; (b) E_d [Author's material]

The sections across the dams confirm these trends. Figs. 10 and 11 show the phreatic surface, the bedrock surface and the surface of sound rock. They also show the dam axis and the loading-berm axes. Fig. 11 also shows the base of the dam. The numbered zones are the dam materials. In Fig. 10, zone 1 is hydraulic-fill aeolian sand. Zones 2 and 5 are gravel-rubble soil. Zone 3 is aeolian fill sand. Zone 4 is rock fill. In Fig. 11, zone 4 is gravel-rubble soil. Zone 5 is aeolian sand. Zone 6 is sandy loam and sand. Zone 7 is rock fill.

On the river-bed dam, ν is laterally uniform (Fig. 10). Most of the dam body lies below the phreatic surface. Over most of the section, ν is therefore 0.46-0.475. Lower values (0.22-0.24) occur only in the unsaturated zone near the crest. In the rock fill at the downstream toe, ν is 0.30-0.33. The section shows no local anomaly of ν. There is no indication of disturbed fill.

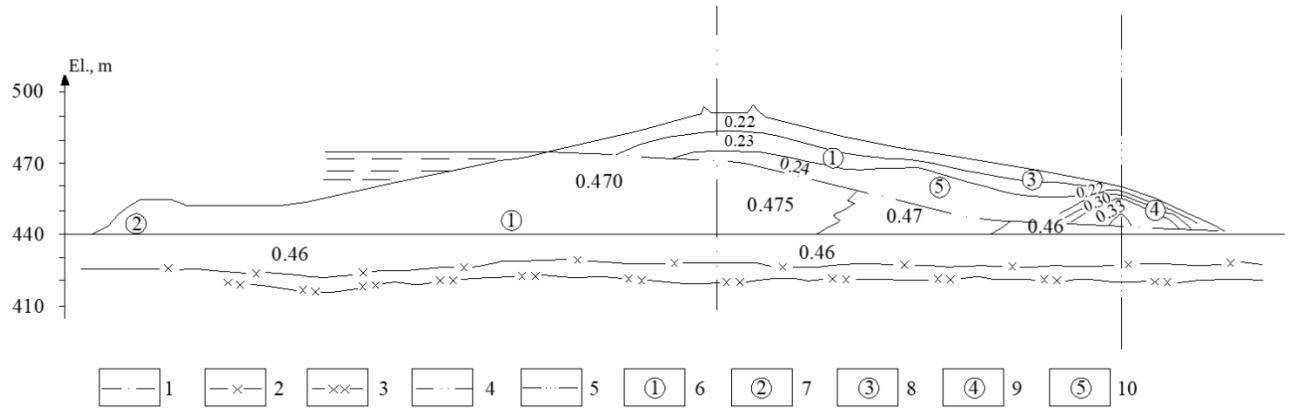

Figure 10 - Distribution of ν across the river-bed dam [Author's material]

https://doi.org/10.51488/1680-080X/2026.3-21

On the ravine dam, V_p was mapped across Sections PK 2+39.5 and PK 1+89.5 (Fig. 11). In the unsaturated zone, V_p increases with depth from 0.4 to 0.8 km/s. Below the phreatic surface, it rises to 1.6-2.2 km/s. In the underlying rock, it reaches 2.4-4.0 km/s. The velocity contours follow the dam zoning. They show no local low-velocity zone. The profiles obtained here describe the dam materials. The recorded earthquake response of the dam [16] describes the structure as a whole. Together, these data can be used to calibrate a numerical model of the dam.

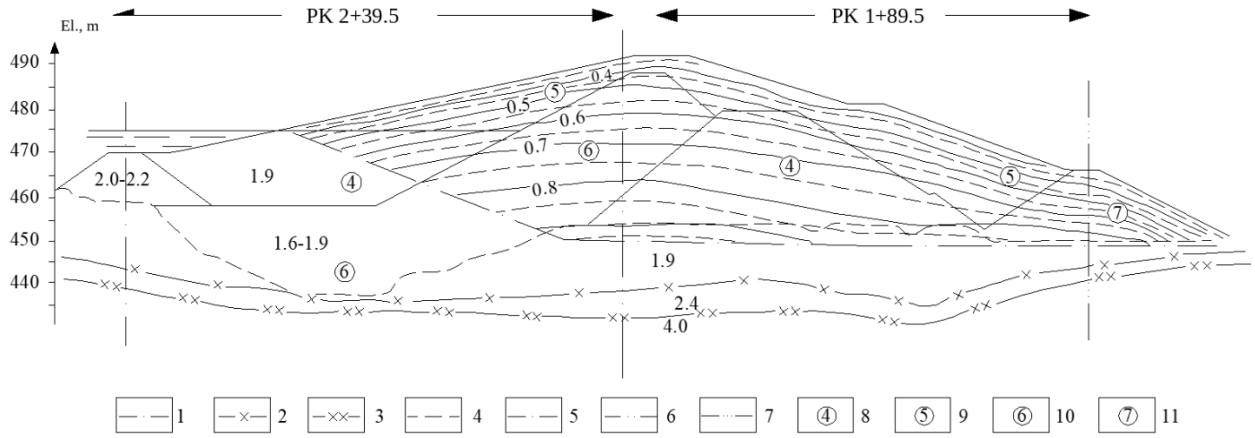

Figure 11 - Distribution of V_p across the ravine dam [Author's material]

3.4 Rock abutment

The abutment rock has two conditions (Table 5). The outcrop body is fractured quartz porphyry. Its compressive strength is 147 MPa. Its elastic modulus is 7.4 GPa. The upper 2 m are intensely fractured. Here, the compressive strength is 71 MPa. This is about half the outcrop-body value. The elastic modulus falls more sharply, to 2.9 GPa. This is about 40 % of the outcrop-body value. The Poisson's ratio rises from 0.30 to 0.35. The friction angle falls from 35.8° to 33.0°. Cohesion falls from 0.20 to 0.10 MPa.

Since 1976, the abutment benchmarks have moved vertically by -1 to +3 mm. These movements are within the levelling accuracy. The positive values are probably due to thermal expansion of the rock.

The rock deep inside the abutment has low permeability. Its specific water absorption is 0.01-0.1 L/min. Its hydraulic conductivity is 0.03-0.30 m/day. Piezometric levels in this zone are stable. They respond weakly to the headwater level.

Near the grout curtain, the levels are high. They usually exceed the headwater level. In P-1 (Section 2-2) and other piezometers, this reflects standing water in the sumps. Near the penstocks, P-2 (Section 5a-5a) and P-5 (Section 8-8) show level changes of several metres within a month. The headwater level varies much less. These changes are therefore not caused by the reservoir. Near the drainage adit, the head drops sharply over a short distance. The adit thus continues to intercept seepage.

No deterioration of rock strength or deformability was detected during operation. The stability of the abutment therefore meets the design assumptions.

Table 5. Physico-mechanical properties of the rock abutment [Author's material]

Rock condition	ρ natural, g/cm³	ρ saturated, g/cm³	Compressive strength, MPa	E, GPa	ν	φ, °	c, MPa
Fractured quartz porphyry (outcrop body)	2.59	2.61	147	7.4	0.30	35.8	0.20
Intensely fractured quartz porphyry (upper 2 m)	2.57	2.59	71	2.9	0.35	33.0	0.10

https://doi.org/10.51488/1680-080X/2026.3-21

3.5 Seismic slope-stability analysis

Table 6 gives the stability factors of the upstream and downstream slopes of both dams. It covers the basic (static) combination and the special combination at intensities 7, 8 and 9. The static factors do not depend on seismicity. For the ravine dam, they are 3.03 upstream and 2.40 downstream. For the river-bed dam, they are 2.69 and 2.31.

Seismic loading reduces K_s on every slope. The reduction grows with intensity. On the upstream slope of the ravine dam, K_s is 2.14 at intensity 7, 1.63 at 8 and 1.14 at 9. On its downstream slope, K_s is 2.07, 1.82 and 1.49. On the upstream slope of the river-bed dam, K_s is 2.04, 1.63 and 1.19. On its downstream slope, K_s is 1.95, 1.68 and 1.34.

Table 6. Computed stability factors of the dam slopes [Author's material]

Structure	Load combination	Seismic intensity	Normative K_s	K_s, upstream slope	K_s, downstream slope
Ravine dam	Basic	-	1.32	3.03	2.40
	Special	7	1.18	2.14	2.07
	Special	8	1.18	1.63	1.82
	Special	9	1.18	1.14	1.49
River-bed dam	Basic	-	1.32	2.69	2.31
	Special	7	1.18	2.04	1.95
	Special	8	1.18	1.63	1.68
	Special	9	1.18	1.19	1.34

Figs. 12 and 13 show the critical slip surfaces at intensity 9. This is the governing case. The upstream slope is on the left, and the downstream slope is on the right. Green curves are slip surfaces of the basic combination. Magenta curves are those of the special combination. Each curve is labelled with its centre coordinates, radius r and stability factor K.

Seismic loading shifts the critical circle. On the ravine dam, the radius increases from 96.3 to 121.2 m upstream. Downstream, it increases from 92.4 to 109.2 m. On the river-bed dam, the radius increases from 99.8 to 111.7 m downstream. Upstream, it decreases from 125.9 to 119.6 m.

The numbered zones are the dam materials. In Fig. 12, zone 1 is gravel-rubble soil of borrow pit No. 16 and the supply channel. Zone 2 is aeolian sand of borrow pit No. 3. Zone 3 is the sandy-loam screen. Zone 4 is the rock fill of the loading berms and upstream slope protection. Zone 5 is the sand-grus foundation. In Fig. 13, zones 1 and 3 are aeolian hydraulic-fill sand of borrow pit No. 3. Zone 6 is the alluvial gravel-sand foundation. Zone 7 is the rock fill of the downstream toe. Zone 8 is the fractured quartz porphyry of the foundation.

https://doi.org/10.51488/1680-080X/2026.3-21

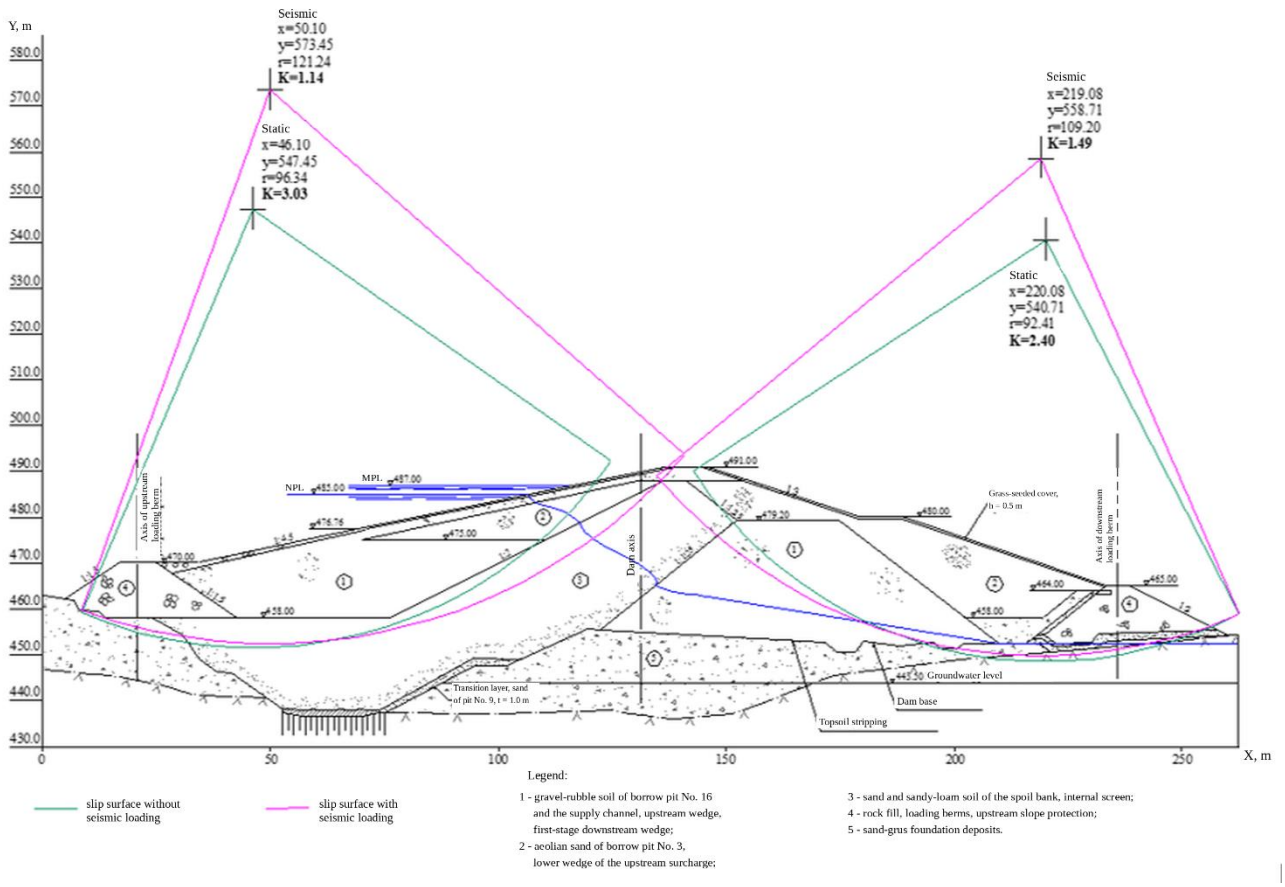

Figure 12 – Slope stability of the ravine dam at seismic intensity 9 [Author's material]

In the basic combination, all slopes exceed the normative minimum of 1.32. The margin is a factor of 1.75 or more. At the current site intensity of 8, all slopes exceed the special-combination minimum of 1.18 by a wide margin. The smallest value is 1.63, on the upstream slopes of both dams.

Intensity 9 is the check level. It is one point above the current site intensity. At this level, the upstream slope of the river-bed dam just meets the requirement, with K_s = 1.19 (Fig. 13). The upstream slope of the ravine dam is the governing case (Fig. 12). Its K_s of 1.14 is 3.4 % below the normative minimum. The pseudo-static method is conservative. A refined dynamic analysis of this slope is nevertheless recommended. The upstream slopes of both dams are the critical elements of the pressure front. They should have priority in monitoring.

https://doi.org/10.51488/1680-080X/2026.3-21

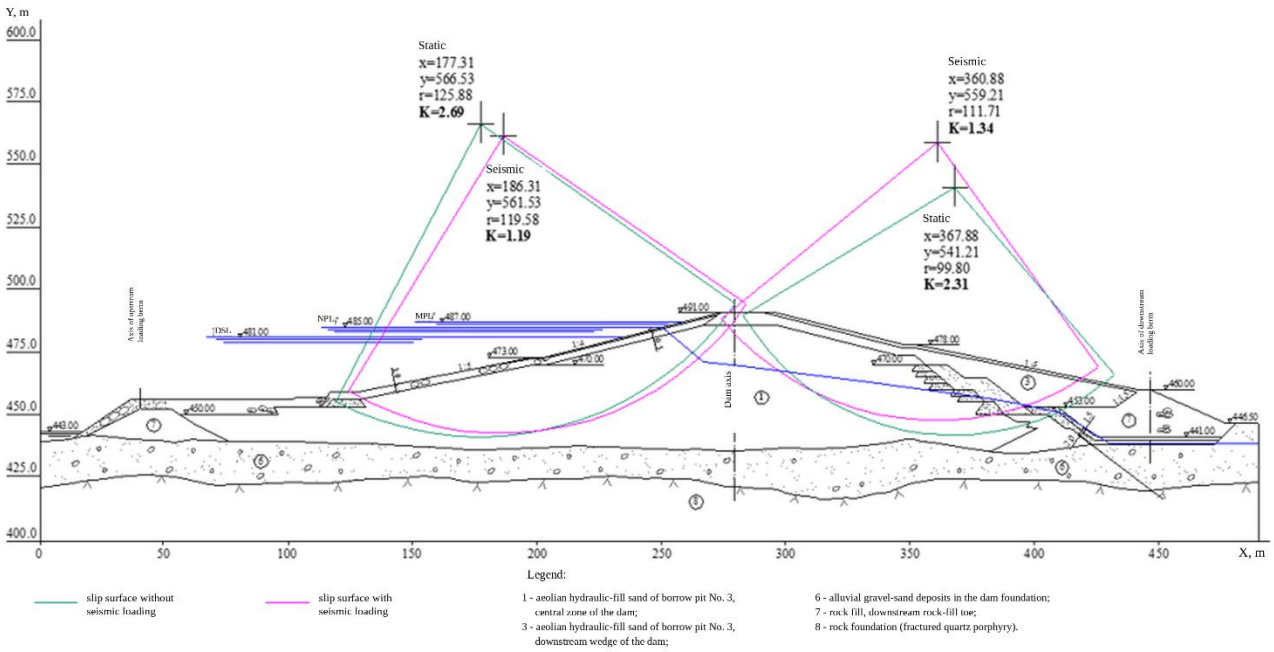

Figure 13 – Critical slip surfaces of the river-bed dam at seismic intensity 9 [Author's material]

4 CONCLUSIONS

T his study assessed the pressure front of the Kapchagay HPP under the revised site seismicity. It used long-term settlement records, current seepage data, dynamic-property profiles, rock properties and a pseudo-static slope-stability analysis. The main conclusions are as follows.

1 . The seepage regime of both dams is stable. On the river-bed dam, heads in the central zone and downstream wedge have changed little for a decade. In all monitored sections, the head decreases from the upstream to the downstream face. The largest head loss occurs in the upstream part of each dam. During the survey, the headwater was about 6.4 m below the normal pool level. Several piezometers in the upstream wedge of the ravine dam were therefore dry.

2. The settlement of both dams is decaying. Over the last two decades, the mean settlement rate was 1.6-2.3 mm/yr on the river-bed dam and 2.06-3.8 mm/yr on the ravine dam. The river-bed dam is at the upper bound of the 1-2 mm/yr stabilisation reference. The ravine dam exceeds it and has not yet reached the stabilisation level. On both dams, the rates decrease with time. The relative compression rate is 0.003-0.004 %/yr on the river-bed dam and 0.005-0.010 %/yr on the ravine dam. Both values are well below 0.02 %/yr. Abrupt steps and rises in some records more likely reflect changes in the observation network than real deformation.

3. Beneath the crest and berm of both dams, V_p, V_s and E_d increase steadily with depth in the unsaturated zone. No anomaly indicating disturbed fill was found. Below the phreatic surface, ν rises to 0.45-0.475. This is typical of saturated soil. At equal depth, the ravine dam is stiffer than the river-bed dam. At 35-40 m, its E_d reaches 1.1-1.2 GPa. This reflects its coarser gravel-rubble soils. These are the first published dynamic-property profiles for the ravine dam. They provide a baseline for future dynamic passports and, together with the recorded seismic response [16], for numerical modelling of the dams.

4. The fractured quartz porphyry of the abutment has a compressive strength of 147 MPa and an elastic modulus of 7.4 GPa. In the intensely fractured upper 2 m, these values fall to 71 MPa and 2.9 GPa. Since 1976, the abutment benchmarks have moved by -1 to +3 mm. These movements are within the levelling accuracy. The rock inside the abutment has a low hydraulic conductivity of 0.03-0.30 m/day. No deterioration of rock properties was detected during operation.

5. In the basic combination, all slopes exceed the normative minimum of 1.32 by a factor of 1.75 or more. At the current site intensity of 8, all slopes exceed the special-combination minimum

https://doi.org/10.51488/1680-080X/2026.3-21

of 1.18. The smallest value is 1.63, on the upstream slopes of both dams. At the check intensity of 9, the upstream slope of the river-bed dam just meets the requirement, with K_s = 1.19. The upstream slope of the ravine dam has K_s = 1.14. This is 3.4 % below the normative minimum.

Overall, the pressure front meets the stability and serviceability requirements at the current site intensity of 8. The safety margin decreases with seismic intensity. The upstream slopes of both dams are the critical elements and should have priority in monitoring. The survey data were obtained at a reduced headwater level. The next update of the dynamic passports should therefore include phreatic curves at higher reservoir levels. It should also include a refined dynamic analysis of the upstream slope of the ravine dam. The automated monitoring system should be restored before this update. During the survey, 23 of the 51 pressure transducers, both level gauges and one joint gauge were out of service.

REFERENCES

1. **Pueppke, S.G., Zhang, Q., Nurtazin, S.T.** (2018). Irrigation in the Ili River Basin of Central Asia: From ditches to dams and diversion. Water 10(11), 1650. https://doi.org/10.3390/w10111650
2. **Vologdin, N.V.** (1972). The Kapchagai hydroelectric station on the Ili river. Gidrotekh. Stroit. 5, 1-7. (In Russian)
3. **Abakanov, T., Begalinov, A., Abakanov, A.** (2016). Seismic stability of tunnels at the Kapchagai hydropower plant. Soil Mech. Found. Eng. 53, (60-65). https://doi.org/10.1007/s11204-016-9365-9
4. **SN RK 3.04-01-2023.** Hydraulic Structures; Committee for Construction and Housing and Utilities, Ministry of Industry and Construction of the Republic of Kazakhstan: Astana, Kazakhstan, 2023. (In Russian)
5. **Darbre, G.R., Proulx, J.** (2002). Continuous ambient-vibration monitoring of the arch dam of Mauvoisin. Earthq. Eng. Struct. Dyn. 31(2), 475-480. https://doi.org/10.1002/eqe.118
6. **Sevim, B., Altunışık, A.C., Bayraktar, A.** (2013). Structural identification of concrete arch dams by ambient vibration tests. Adv. Concr. Constr. 1(3), 227-237. https://doi.org/10.12989/acc.2013.1.3.227
7. **Jafari, M.K., Davoodi, M.** (2006). Dynamic characteristics evaluation of Masjed Soleiman Dam using in situ dynamic tests. Can. Geotech. J. 43(10), 997-1014. https://doi.org/10.1139/t06-059
8. **Verret, D., LeBoeuf, D.** (2022). Dynamic characteristics assessment of the Denis-Perron dam (SM-3) based on ambient noise measurements. Earthq. Eng. Struct. Dyn. 51(3), 569-587. https://doi.org/10.1002/eqe.3580
9. **Ilgac, M., Athanasopoulos-Zekkos, A., Nweke, C.C., Ktenidou, O.-J., Peterson, K., Kayen, R.E.** (2025). Embankment vibration characteristics using ground motion records and ambient noise measurements, Briones Dam, California. Soils Found. 65, 101664. https://doi.org/10.1016/j.sandf.2025.101664
10. **ICOLD** (2018). Dam Surveillance Guide; Bulletin 158; CRC Press: London, UK. ISBN 978-1-138-49020-8.
11. **Moldamuratov, Zh.N., Ilyassova, K.I., Kareken, G.T., Shanshabayev, N.A., Orazov, S.E., Vatin, N.I., Yessenkeldin, A.M.** (2026). Non-destructive ground-penetrating radar survey of hydraulic structures using the OKO-3 GPR to detect hidden defects and assess technical condition. Bulletin of the Kazakh Leading Academy of Architecture and Civil Engineering 1(99), 417-440. https://doi.org/10.51488/1680-080X/2026.1-28
12. **Moldamuratov, Zh.N., Ilyassova, K.I., Vatin, N.I., Kareken, G.T., Shanshabayev, N.A., Sadyrov, R.K., Bryantsev, A.A., Tashmukhanbetova, I.B., Yessenkeldin, A.M.** (2026). Assessment of the technical condition of concrete and reinforced concrete hydraulic structures using 3D ultrasonic tomography. Bulletin of the Kazakh Leading Academy of Architecture and Civil Engineering 1(99), 441–463. https://doi.org/10.51488/1680-080X/2026.1-29

https://doi.org/10.51488/1680-080X/2026.3-21

13. **Foti, S., Hollender, F., Garofalo, F., Albarello, D., Asten, M., Bard, P.-Y., Comina, C., Cornou, C., Cox, B., Di Giulio, G.** (2018). Guidelines for the good practice of surface wave analysis: A product of the InterPACIFIC project. Bull. Earthq. Eng. 16(6), 2367-2420. https://doi.org/10.1007/s10518-017-0206-7
14. **Kramer, S.L.** (1996). Geotechnical Earthquake Engineering; Prentice Hall: Upper Saddle River, NJ, USA.
15. **Lapin, V., Aldachov, Y., Makish, N., Aldachov, S., Ali, A.** (2023). Dynamic and spectral characteristics of the Kapchagay HPP dam. In Smart Geotechnics for Smart Societies; CRC Press: London, UK; pp. 2286-2291. https://doi.org/10.1201/9781003299127-353
16. **Moldamuratov, Zh., Kareken, G., Ilyassova, K., Abyieva, G., Shanshabayev, N., Lapin, V.; Tasmaganbetova, A., Tukhtamisheva, A.** (2026). Seismic response and frequency-dependent amplification of the Kapchagay earthfill dam from instrumental bedrock-to-crest earthquake records. ES Mater. Manuf. https://doi.org/10.30919/mm2547
17. **Abakanov, T.** (2020). Fundamentals of ensuring geodynamic (seismic) safety of buildings and structures at developed mineral deposits [Osnovy obespecheniya geodinamicheskoi (sesimicheskoi) bezopasnosti zdanii I soorujenii na razrabatyvaemyh mestorozhdeniyah poleznyh iskopaemyh]. Bulletin of the Kazakh Leading Academy of Architecture and Civil Engineering 3(77), 85-90. https://doi.org/10.51488/1680-080X/2020.3-10 (In Russian)
18. **Ilyassova, K., Vatin, N., Tashmukhanbetova, I., Moldamuratov, Zh.** (2025). Analysis of degradation mechanisms and justification of repair technologies for concrete hydraulic structures. Bulletin of the Kazakh Leading Academy of Architecture and Civil Engineering 3(97), 90-107. https://doi.org/10.51488/1680-080X/2025.3-07
19. **Kuznetsova, I.A., Kasenzhanov, M.M.** (2023). Geodetic works to determine vertical movements at the Zhambyl geodynamic polygon [Geodezicheskie raboty po opredeleniu vertikalnyh smexhenii na zhambylskom geodinamicheskom poligone]. Bulletin of the Kazakh Leading Academy of Architecture and Civil Engineering 2(88), 260-269. https://doi.org/10.51488/1680-080X/2023.2-26 (In Russian)
20. **Baymakhan, R.B., Rysbaeva, A.K., Seinasinova, A.A., Baymakhan, A.R., Kadirova, Zh.B.** (2020). Mathematical modelling and investigation of the landslide condition of the Shym Bulak mountain slope [Matematicheskoe modelirovanie I issledovanie opolznevogo sostoyaniya sklona gory Shymbulak]. Bulletin of the Kazakh Leading Academy of Architecture and Civil Engineering 3(77), 259–264. https://doi.org/10.51488/1680-080X/2020.3-35 (In Russian)
21. **Apshikur, B., Imankulova, A.S., Kunanbayev, A.K., Alimkulov, M.M., Lesov, K.** (2025). Development of an effective method for strengthening weak foundations of railway embankments. Bulletin of the Kazakh Leading Academy of Architecture and Civil Engineering 4(98), 108–128. https://doi.org/10.51488/1680-080X/2025.4-07
22. **SP RK 2.03-30-2017.** Construction in Seismic Zones (as amended on 12 August 2025); Committee for Construction and Housing and Utilities: Astana, Kazakhstan, 2017. (In Russian)
23. **P 87-2001.** Recommendations for Field Observations of Settlements of Earth Dams; VNIIG im. B.E. Vedeneeva: St. Petersburg, Russia, 2001. (In Russian)
24. Rules for the Technical Operation of Power Plants and Networks. Approved by Order of the Minister of Energy of the Republic of Kazakhstan No. 247 of 30 March 2015; registered No. 11066. Available online: https://adilet.zan.kz/rus/docs/V1500011066 (In Russian)

https://doi.org/10.51488/1680-080X/2026.3-21

FUNDING

The study was carried out with the financial support of the Science Committee of the Ministry of Science and Higher Education of the Republic of Kazakhstan within the framework of research project No. AP23487624.

CONFLICT OF INTEREST

The authors declare no conflict of interest.

ARTIFICIAL INTELLIGENCE STATEMENT

During the preparation of this manuscript, the authors used artificial intelligence tools solely for language editing, grammar checking, and text improvement. All scientific content, interpretations, analyses, and conclusions remain the responsibility of the authors.

AUTHOR CONTRIBUTIONS

Kareken G.T. – Conceptualization, Methodology, Investigation, Formal Analysis, Writing - Original Draft.
Vatin N.I. – Supervision, Validation, Review & Editing.
Shanshabayev N.A. - Formal Analysis, Review & Editing.
Bryantsev A.A. - Formal Analysis, Review & Editing.
Orazov S.Ye. - Formal Analysis, Review & Editing.

INFORMATION ABOUT THE AUTHORS

• Kareken Gulfairuz Talgatkyzy
• PhD student
• International Educational Corporation
• 050043, Almaty, Kazakhstan
• E-mail address: gulfairuz_1997@mail.ru
• ORCID ID: https://orcid.org/0000-0002-9459-3980

• Vatin Nikolai Ivanovich
• PhD, professor
• Peter the Great St. Petersburg Polytechnic University (SPbPU)
• 195251, St. Petersburg, Russia
• E-mail address: vatin_ni@spbstu.ru
• ORCID ID: https://orcid.org/0000-0002-1196-8004

• N.A. Shanshabayev
• PhD
• LLP «StroyTechExpertiza»
• Taraz, Kazakhstan
• E-mail address: nucho91@mail.ru
• ORCID ID: https://orcid.org/0000-0003-4930-0488

https://doi.org/10.51488/1680-080X/2026.3-21

• A.A. Bryantsev
• PhD
• LLP «RAS Engineering Research Institute»
• Almaty, Kazakhstan
• E-mail address: a.briantcev@kazgasa.kz
• ORCID ID: https://orcid.org/0000-0002-6932-8202

• S.Ye.Orazov
• PhD student
• International Educational Corporation
• 050043, Almaty, Kazakhstan
• E-mail address: sa.orazov@kazgasa.kz
• ORCID ID: https://orcid.org/0009-0001-8764-5869

Received: 15 July 2026
Revised: 05 August 2026
Accepted: 28 September 2026

https://doi.org/10.51488/1680-080X/2026.3-21